Assembly of Metal Nanoparticle Arrays Using Molecular Bridges

by Dan Feldheim

This article reviews recent work by our group aimed at organizing metal nanoparticles into symmetrically and spatially well defined architectures. The impetus for this work is two-fold. First, metal nanoparticle aggregates display rich optical behaviors that are distinctly different from a corresponding collection of individual particles or the extended solid. A range of fundamentally interesting new materials can thus be constructed from a single inorganic building block (gold, silver nanoparticles) simply by controlling such parameters as aggregate size, shape, and interparticle distance. Indeed, nanoparticle linear and nonlinear optical properties, hyperpolarizabilities, and electric field enhancement factors have been found to depend strongly on these parameters.[1] In addition to generating significant fundamental interest, applications of nanoparticle-based materials are emerging, in which collective nanoparticle optical properties are exploited for colorimetric, surface-enhanced Raman (SERS) and surface plasmon resonance (SPR) bioassays.[2] A number of home pregnancy and drug test kits based on the optical properties of gold nanoparticles are already available commercially.[3]

A second theme that has emerged in nanoparticle research more recently pertains to their electrical characteristics. Individual 5 nm diameter particles have been wired up and shown to have properties useful in fabricating nanoscale analogues of traditional electronic device components such as transistors and tunnel diodes.[4] Less conventional forms of computing based on assemblies of nanoparticles have also been proposed. These schemes, coined quantum cellular automata (QCA), rely on electrostatic coupling between square planar assemblies of metal dots.[5] However, the implementation of QCA at room temperature will require dots smaller than 10 nm in diameter. Arranging such small structures into well defined "integrated" systems is difficult using most forms of lithography (*e.g.*, photo, electron beam, scanning probe lithographies). Chemical self-assembly likely will become an important tool for the realization of integrated nanoscale electronics. In this respect, metal nanoparticles are potentially powerful minimum device components because their surfaces can be modified using a number of well developed and relatively routine chemical attachment strategies.

With these fundamentally interesting and technologically important goals in mind, we sought new protocols for assembling nanoparticles into covalently linked arrays. We chose to begin our studies by linking gold and silver particles together to form relatively small aggregates—dimers, trimers, and

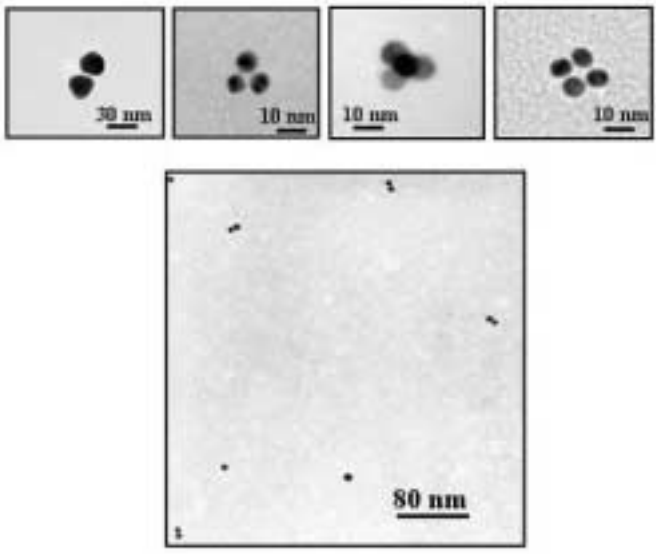

FIG. 1. Transmission electron micrographs of gold nanoparticle arrays assembled using molecules (from top left to right): IC, IIIb, II, and IV. Bottom image shows an expanded view of gold nanoparticle dimers.

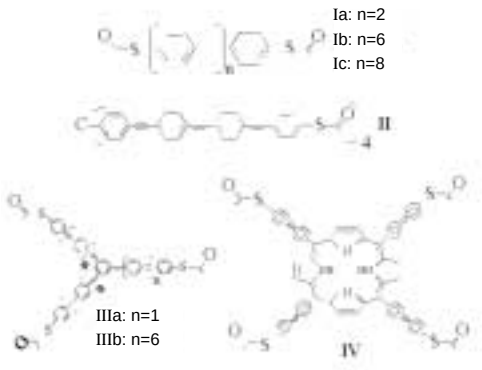

SCHEME 1. Phenylacetylene structures used as nanoparticle linkers.

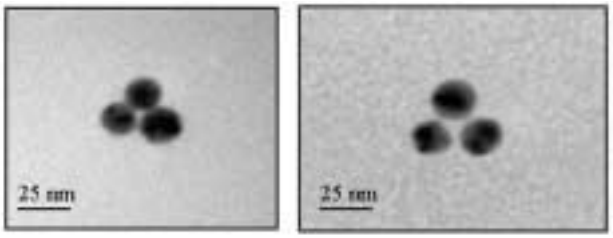

FIG. 2. Transmission electron micrographs of gold nanoparticle arrays assembled using molecules IIIA (left) and IIIB (right).

tetramers—with well-defined symmetries and interparticle distances. With these structures in hand we are addressing questions such as the following ones. How do nanoparticles communicate electronically and electromagnetically as a function of interparticle distance, array symmetry, and bridge chemistry? How are the electronic properties of a molecular bridge perturbed by the surrounding nanoparticles? Can molecules be chosen to act as "chemical gates" of electron transport between particles? As described below, we found that a variety of organic supermolecules could serve as "templates" for the formation of nanoparticle arrays.

Assembly of Molecularly Bridged Nanoparticle Arrays

Molecular bridges based on phenylacetylene units were chosen as a primary nanoparticle assembly tool because of their rigidity, and the relative ease with which they can be coupled together to form oligomers in a variety of symmetries and lengths (Scheme 1).[6] When mixed slowly over time (1 hr.) with a desired nanoparticle suspension, each thiol end group binds to a single nanoparticle to form a nanoparticle array whose symmetry and interparticle distance is dictated by the molecular bridge. Particle crosslinking and precipitation is avoided by using an excess of nanoparticles relative to molecular bridge. Figure 1 shows transmission electron micrographs (TEM) of gold nanoparticle arrays with $D_{\infty h}$, D_{3h}, D_{4h}, and T_d symmetries. Note that the particles are not fused, but are separated by a distance that we believe is governed by the lengths of the phenylacetylene bridge. Increasing the arm lengths on the trithiol by one phenylacetylene unit, for example, increases the distance between particles (Fig. 2).

An expanded TEM view reveals that the presence of excess monomeric particles in the reaction mixture prevents the formation of extended aggregates (Fig. 1). Indeed, in every case the desired geometry plus unreacted subunits of that structure are found almost exclusively by TEM. For example, dithiols yield particle dimers and monomers, trithiols yield particle trimers, dimers, and monomers, etc. The histograms shown in Fig. 3 illustrate this observation. In general, yields from the as-synthesized reaction mixture range from 30% – 50 % for the dimers and trimers, and 10% – 20% for the tetrahedra and square planar arrays. Enriched fractions of a particular array can be collected by ultracentrifugation in 1 M sucrose. Figure 3 shows an image from a sample that has been purified to contain > 60% of the trimer structure.

Electromagnetic Coupling in Molecularly Bridged Nanoparticle Arrays

The molecularly bridged nanoparticle arrays shown here have enabled the characterization of symmetry and distance dependent electromagnetic coupling between metal particles. Strong interparticle coupling was first demonstrated by UV-visible spectroscopy.[7] Figure 4a, for example, displays visible extinctions of two 30 nm diameter silver particles bridged by progressively shorter phenylethynyl dithiols. Solutions of unlinked silver particles contain a single extinction band centered at 420 nm corresponding to the well-known silver plasmon resonance band. Addition of a 9-unit phenylacetylene bridge caused a slight redshift and absorbance increase of the silver plasmon band. At separation distances corresponding to 7 phenylacetylene units, an extinction at 450 nm was observed with a more well-defined shoulder at 420 nm. Both bands were more intense than the single-particle plasmon band. Further reduction in separation to 3 phenylacetylene units caused no further shift in the low-energy extinction; however, the high-energy shoulder blue shifted to 370 nm and both bands grew in intensity. In addition, a relatively weak extinction was observed at ca. 600 nm.

The visible spectra described above for gold and silver particle dimers are consistent with recent calculations using dipole approximations.[8] Figure 4b presents spectra calculated

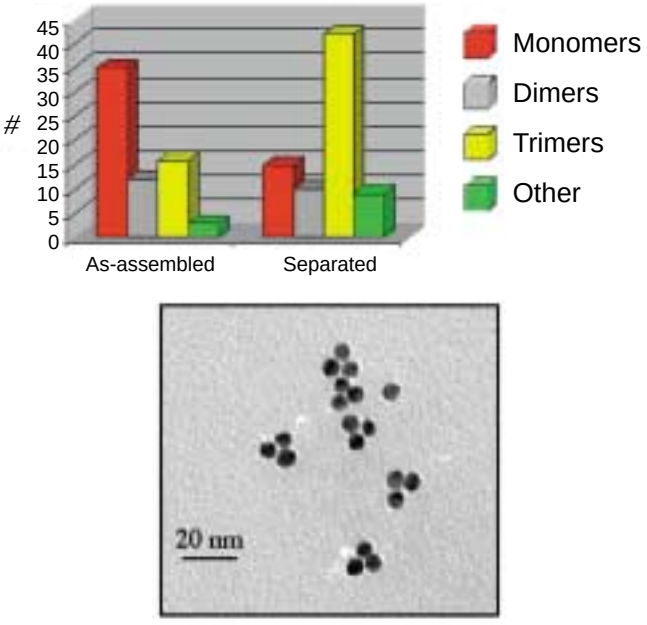

FIG. 3. Top: Histogram showing # of structures observed by TEM after array assembly and following centrifugation in 1 M sucrose. Bottom: TEM image of gold nanoparticle trimers following centrufugation.

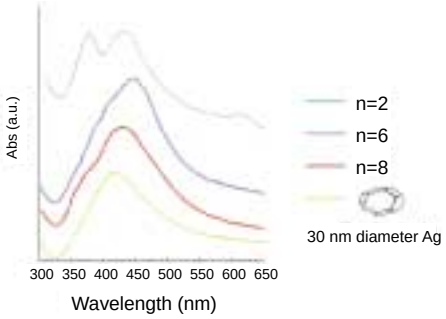

FIG. 4a. UV-visible spectra of 30 nm diameter silver particles (bottom), and phenylacetylene-bridged dimers with n equal to 8, 6, and 2. (Spectra were offset for clarity).

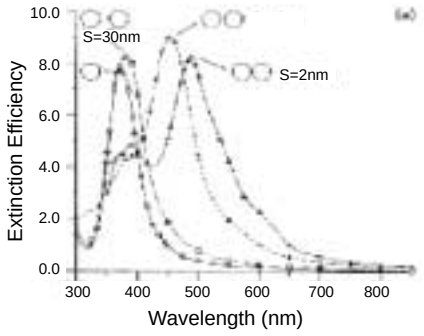

FIG. 4b. Calculated silver particle spectra (from reference 8).

for 60 nm diameter particle dimers as a function of particle separation distance. Note, despite the size difference, the behaviors are qualitatively in agreement; that is, both data sets reveal a red-shift of the single-particle plasmon band, an increase in overall extinction efficiency, growth of a high-energy shoulder (ca. 370 nm), and subsequent appearance of a band at 600 nm as interparticle distance decreases. The bands at 450 nm and 420 nm can be attributed to the longitudinal and transverse plasmon modes, respectively, of the dimer. (The 420 nm band may also contain contributions from quadrupole moments). The feature at 600 nm is as yet unassigned. Disparities between experimental and calculated spectra are likely due to particle size dispersity, the presence of excess monomers, and orientational averaging in solution not accounted for theoretically.

Further information about electromagnetic coupling in metal nanoparticle arrays has been obtained with hyper-Rayleigh scattering spectroscopy (HRS).[9] HRS measures incoherently scattered frequency doubled radiation from a sample of chromophores. HRS differs from other second harmonic techniques in that the frequency doubled light scales as the variance of the orientation with respect to the electromagnetic field. The variance is nonzero even for a randomly oriented sample. Consequently, HRS can be performed on solution suspensions without electric field or other poling techniques. Because HRS effectively measures second harmonic generation, we expected that output signals would be enhanced for noncentrosymmetric nanoparticle trimer or tetrahedral arrays, compared to centrosymmetric monomers and dimers.

Figure 5 shows HRS intensities as a function of the square of the input power for 8 nm diameter gold monomers, dimers, and trimers. Note that noncentrosymmetric gold trimers are relatively high nonlinear scatterers *vs.* centrosymmetric dimers and monomers. Insofar as the conventional molecular first hyperpolarizability (β) holds for these larger structures, β can be used as a marker of electromagnetic communication between particles in an array. Table I reports β^2/atom as a function of interparticle symmetry and distance. All values reported, including those for the centrosymmetric monomers and dimers, are as large or larger than the best molecular chromophores. Intense HRS from gold monomers is thought to result from higher-order moments. However, by arranging particles into the noncentrosymmetric trimer structure, we have observed HRS intensities up to 30 times those of the monomeric particles.

Also reported in Table I is the depolarization ratio, D (ratio of vertically *vs.* horizontally polarized HRS). Within the context of molecular scatterers, D reports on the symmetry of the scatterers. Theoretically, D equals 2.0 for scatterers with the symmetries of the monomers and dimers, and 1.5 for the trimers. These values are in accord with those measured experimentally, a result which suggests that a majority of the nanoparticle arrays in solution exist in the geometries observed by TEM.

Finally, HRS has proven to be a sensitive measure of the distance dependence of electromagnetic communication between particles in an array. For the two trimer assemblies measured to date, β^2/atom decreases with increasing interparticle separation distance (and thus decreasing electromagnetic communication). In contrast, no distance dependence was found for the dimer arrays, suggesting that particles are acting as individual, rather than collective, scatterers.

Future Directions in Organized Nanoparticle Assemblies

For well over 1,000 years metal nanoparticles have been exploited for their colorful and intense visible light extinctions. Cr, Co, Au, Ag, and Mo nanoparticles have been found in paintings and stained glass created by ancient Mayan and European civilizations. In fact the oldest known object incorporating gold nanoparticles is thought to be the Lycurgus chalice dating back to 5th century Rome.

The optical properties of metal nanoparticles continue to fascinate scientists today. Our theoretical understanding of nanoparticle optical properties has improved dramatically since Maxwell-Garnett first calculated in 1904 the colors observed for spherical gold particles as a function of interpar-

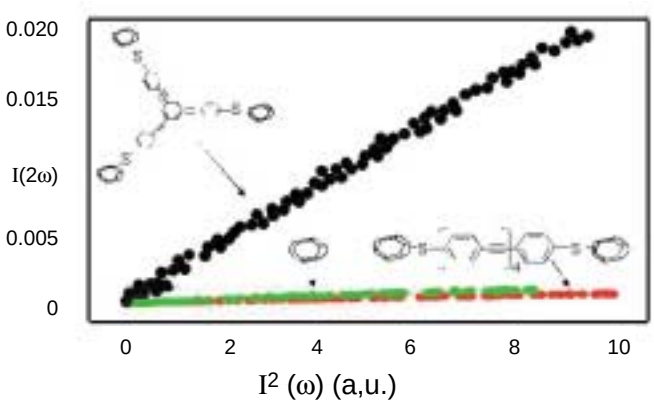

FIG. 5. Relative HRS intensity of 8 nm diameter gold particle trimers (IIIB), dimers (IB), and monomers.

Table I. HRS data for gold Nanoparticles and Arrays.

Particle Array; Molecular Bridge	β^2/atom (10^{-30} esu)	Depolarization Ratio ($\beta v/\beta h$)
Trimer; IIIA	3800±410	1.6±0.07
Trimer; IIIB	2700±330	1.6±0.02
Dimer; IA	1300±160	1.9±0.2
Dimer; IB	1100±120	1.9±0.2
Dimer; IC	1530±150	2.1±0.1
Monomer	1800±200	1.8±0.04

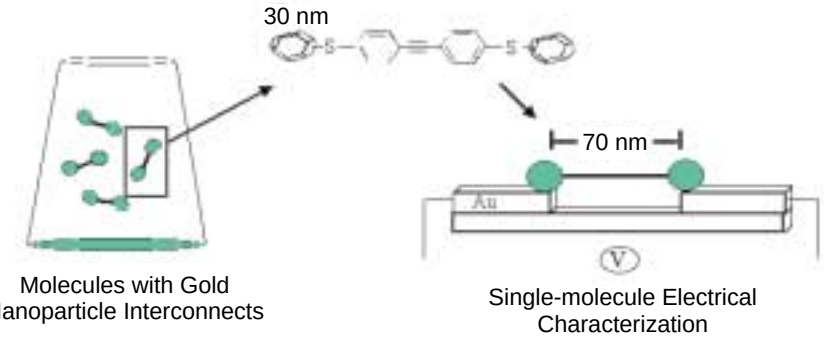

SCHEME 2: Nanoparticles in the future may be useful interconnects between the molecular (5 nm) and photolithographic (100 nm) length scales.

ticle distance. Yet despite a century of extensive theoretical and experimental research, a detailed understanding of nanoparticle aggregate size and shape effects on optical behaviors such as SERS and second harmonic generation has been largely elusive. This is in part because to date few routine and reliable methods have been developed for organizing nanometer-sized particles into spatially complex architectures.

The work reviewed here illustrates that appropriately designed organic supermolecules can serve as useful templates for organizing nanoparticles into covalently bridged arrays. These "molecules of nanoparticles" can be used to test long-standing theories of dipole coupling and electric field enhancements between metal particles. Clearly, a great deal of fundamental nanostructure physics will be uncovered in the future as workers in the field develop new methods for organizing particles into spatially complex arrangements.

In the future, molecularly bridged metal nanoparticle arrays may also serve as useful interconnects between single molecules and macroscopic electrical contacts. Establishing direct electrical connections between gold contacts and individual organic molecules has to date suffered from ambiguities associated with knowing the true identity of the molecule which has "assembled itself" between contacts, and the number, orientation, and contact chemistry of molecules in the gap. The assembly of potential molecular electronic device candidates between metal nanoparticles allows one to characterize these parameters prior to electrical characterization (via solution phase spectroscopies; Scheme 2). An individual nanoparticle array could subsequently be assembled in the gap between macroscale contacts and the number of molecules in the gap inferred by locating their nanoparticle interconnects with TEM, SEM, or AFM—techniques that cannot be used on individual molecules themselves. Moreover, nanoparticle interconnects may also provide some relief from problems arising from fan out. Fabricating 2- or 3- terminal contacts separated by molecular length scales (*e.g.*, sub-10 nm) is a daunting task for even electron beam lithography. However, a 10 nm long molecule connected to two 30 nm diameter gold particles pushes the minimum gap distance required to ca. 70 nm, a much more realistic fabrication dimension. Wiring up the molecularly bridged nanoparticle arrays described above for electrical characterization is a major focus of our current research efforts. ■

Acknowledgments

I am indebted to a number of talented, creative, and energetic people who performed the research described above: Dr. Louis Brousseau, James Novak, Stella Marinakos, Dr. Buford Lemon, Dr. Fred Vance, Robert Johnson, Professor Joseph Hupp, and Dr. Wallace Ambrose. I also thank the generous support of this work by NSF, ONR, the Arnold and Mable Beckman Foundation, and the David and Lucille Packard Foundation.

References

1. (a) G. Chumanov, K. Sokalov, B. Gregory, and T. M. Cotton, *J. Phys. Chem.*, **99**, 9466 (1995); (b) F. W. Vance, B. I. Lemon, J. T. Hupp, *J. Phys. Chem.*, **102**, 10091 (1998).
2. (a) C. A. Mirkin, R. L. Letsinger, R. C. Mucic, J. J. Storhoff, *Nature*, **382**, 607 (1996); (b) L. He, M. D. Musick, S. R. Nicewarner, F. G. Salinas, S. J. Benkovic, M. J. Natan, and C. D. Keating, *J. Am. Chem. Soc.*, **122**, 9071 (2000).
3. www.conceptionstore.com
4. D. L. Feldheim and C. D. Keating, *Chem. Soc. Rev.*, **27**, 1 (1998).
5. C. S. Lent and P. D. Tougaw, *J. Appl. Phys.*, **74**, 6227 (1993).
6. J. Zhang, J. S. Moore, Z. Xu, amd R. A. Aguirre, *J. Am. Chem. Soc.*, **114**, 2273 (1992).
7. J. P. Novak and D. L. Feldheim, *J. Am. Chem. Soc.*, **122**, 3979 (2000).
8. T. Jensen, L. Kelly, A. Lazarides, and G. C. Schatz, *J. Cluster Sci.*, **10**, 295 (1999).
9. J. P. Novak, L. C. Brousseau III, F. W. Vance, R. C. Johnson, B. I. Lemon, J. T. Hupp, and D. L. Feldheim, *J. Am. Chem. Soc.*, **122**, 12029 (2000).

About the Author

Dan Feldheim *earned a bachelor's degree in chemistry in 1990 working in Professor Kevin Ashley's lab at San Jose State University and a PhD degree at Colorado State University in 1995 with Professor C. Michael Elliott. He became interested in chemical methods of assembling nanoscale electronic devices and solar cells as a postdoctoral fellow in Professor Thomas Mallouk's lab at Pennsylvania State University. He moved to North Carolina State University in 1997 where he is an associate professor of chemistry.*